applied sciences

MDPI

Article

Plastic Waste to Carbon Adsorbent: Activation with Sodium Carbonate and Functionalization with Citric Acid

Ledicia Pereira [1], María Ángeles Martín-Lara [1,*], Guillermo Garcia-Garcia [1], Concepción Calvo [2,3], Tatiana Robledo [2,3], Rafael R. Solís [1,*] and Mónica Calero [1]

[1] Department of Chemical Engineering, University of Granada, 18071 Granada, Spain; lpereira@ugr.es (L.P.); guillermo.garcia@ugr.es (G.G.-G.); mcaleroh@ugr.es (M.C.)
[2] Department of Microbiology, University of Granada, 18071 Granada, Spain; ccalvo@ugr.es (C.C.); trobledo@ugr.es (T.R.)
[3] Environmental Microbiology Group, Institute of Water Research, University of Granada, 18071 Granada, Spain
* Correspondence: marianml@ugr.es (M.Á.M.-L.); rafarsolis@ugr.es (R.R.S.)

Featured Application: Plastic waste can be valorized into activated carbon whose functionalization with citric acid affects the chemical surface and the adsorption uptake of contaminants in water.

Abstract: Plastic waste management is currently a challenge of great importance. The valorization of non-recyclable fractions into carbonaceous adsorbents is an interesting strategy that promotes the circular economy. In this work, a waste-to-adsorbent strategy was pursued with the char from plastic pyrolysis. The char (non-porous, surface area ~3 m^2 g^{-1}) was activated with chemical activation, with sodium carbonate boosting the textural properties (surface area ~418 m^2 g^{-1}, pore volume 0.436 cm^3 g^{-1}), triggering the formation of activated carbon with a large mesoporosity (71%). X-ray photoelectron spectroscopy and thermal programmed desorption characterization confirmed the enrichment of the surface with carboxylic groups by treatment with citric acid, with a slight loss of textural properties. The activated carbon showed an enhanced adsorption uptake of lead in water (~52 mg g^{-1} functionalized vs. ~37 mg g^{-1} non-functionalized) and limited influence on the adsorption of acetaminophen. The preparation costs and the consumption cost per unit of removed pollutants confirm the benefits of the activation and functionalization of the original carbonaceous precursor. However, the possible metal lixiviation from plastic additives and the environmental impact according to a life cycle assessment still make this kind of valorization strategy controversial.

Keywords: plastic waste char; activated carbon; sodium carbonate activation; citric acid modification; water contaminant removal; characterization; economic and environmental assessment

Academic Editor: Marco Carnevale Miino

Received: 30 December 2024
Revised: 3 February 2025
Accepted: 4 February 2025
Published: 6 February 2025

Citation: Pereira, L.; Martín-Lara, M.Á.; Garcia-Garcia, G.; Calvo, C.; Robledo, T.; Solís, R.R.; Calero, M. Plastic Waste to Carbon Adsorbent: Activation with Sodium Carbonate and Functionalization with Citric Acid. *Appl. Sci.* **2025**, *15*, 1634. https://doi.org/10.3390/app15031634

1. Introduction

Effective waste management is essential for preserving environmental sustainability and safeguarding public health [1]. Poor waste disposal practices, especially concerning plastics, significantly contribute to land and water pollution, disrupt ecosystems, and pose severe risks to wildlife [2]. Plastic pollution has become a global crisis, with millions of tons of plastic waste entering oceans and landfills annually, where it can persist for centuries [3]. This pollution not only endangers marine life but also breaks down into microplastics, infiltrating food chains and adversely affecting human health [4]. As populations and

consumption levels continue to rise, it is increasingly urgent to address plastic waste through improved waste management systems to mitigate long-term ecological damage and reduce greenhouse gas emissions [5].

One promising strategy for mitigating plastic pollution is its conversion into activated carbon, a highly porous material with excellent adsorptive properties that can be used to remove contaminants from water [6–12]. Activated carbon is typically produced by carbonizing organic material and subsequently activating it using either physical or chemical methods [11–13]. Physical activation involves exposing the carbonized material to gases, such as steam or carbon dioxide, at high temperatures (800–1100 °C), which enhances pore formation [14]. In contrast, chemical activation entails impregnating the carbon precursor with activating agents, often resulting in activated carbon with a higher surface area and larger pore volume compared to physical activation [15,16]. The preparation of activated carbon from diverse plastic waste has been largely investigated. Commonly, specific items or simple polymeric formulas are addressed [7,11,17]. For instance, caps, bottles, or bags have been successfully transformed into activated carbon with competitive textural and chemical properties for adsorption applications [9,11]. The use of complex plastic mixtures, such as those reported in the rejection fraction of plastic waste management plants, has been less explored due to the challenges that must be tackled [10].

Among various chemical agents, KOH is widely used for producing activated carbon with an enhanced porosity and surface area [18]. In addition to KOH, other chemical agents such as H_3PO_4, $ZnCl_2$, NaOH, and K_2CO_3, among others, are also commonly used in the production of activated carbon [19]. Among these activating agents, Na_2CO_3 has emerged as an environmentally friendly alternative, offering a balance between efficiency and ecological impact. This relatively mild agent is effective for developing mesoporosity, which is ideal for the retention of larger molecules.

The activation of materials using Na_2CO_3 has been the focus of various studies in recent years, primarily targeting the production of activated carbon [20,21] for a variety of applications, including the removal of heavy metals [22,23] and organic pollutants [24], and in the development of alkali-activated electrodes [25,26], binders in geopolymers [27], and construction materials [28]. The use of Na_2CO_3 in the alkali activation of high-carbon biomass fly ash demonstrates that increasing the Na_2CO_3/Na_2SiO_3 ratio improved the compressive strength and density of the resulting materials [21]. The adsorption capacity of activated carbon produced from biological materials, such as rice husk [23,29] and oil palm fronds [20,30], has also been investigated. These studies demonstrate that chemical activation with Na_2CO_3 enhances the porosity and specific surface area of activated carbon [26,29], resulting in greater adsorption efficiency for pollutants such as heavy metals, such as Ni [31] or Pb [32], and organic dyes [24,33,34]. Optimizing parameters like activation temperature and the ratio of sodium carbonate to raw materials is essential to maximize adsorption capacity. Several articles compare different activation methods, emphasizing that chemical activation with Na_2CO_3 offers advantages over other activators due to the lower corrosion if compared to alkalis and to safer management in real applications [20,35]. For example, using Na_2CO_3 to produce activated carbon from wastepaper resulted in materials with superior properties for adsorbing dyes like methylene blue [33]. The use of Na_2CO_3 is not limited to biomass-derived materials. The activation of chars obtained from post-consumer mixed plastic waste proved that Na_2CO_3-activated carbon (Na_2CO_3-AC) exhibits superior performance in the adsorption of heavy metals such as Pb (40 mg g^{-1}), Cd (13 mg g^{-1}), and Cu (12 mg g^{-1}) [22]

The optimization of activation processes and the exploration of new feedstock sources remain areas of ongoing interest, promising a bright future for the use of sustainable materials in various industrial applications. Furthermore, integrating chemical activation

methods can significantly mitigate environmental issues, making Na_2CO_3 activation a valuable option in the circular economy and developing cleaner technologies. In addition to Na_2CO_3 activation, modifying activated carbon with citric acid (CA) has gained attention for further improving its adsorption capabilities. Citric acid is a biodegradable, non-toxic organic compound that introduces carboxyl groups to the carbon surface, making citric acid-modified materials suitable for a wide range of applications, particularly for water treatment strategies [36–43]. For instance, citric acid-based residues were employed to produce activated carbon formulas with a superior adsorption uptake of volatile organic compounds such as ethyl acetate [38]. Acid citric can be used to add carboxyl groups onto the surface of the adsorbent, which improves the binding potential of organic adsorbates such as metolachlor, raising the uptake of the non-treated adsorbent from ~51 mg L^{-1} to ~74 mg L^{-1} following citric acid treatment [40]. Citric acid can be used as a green cross-linker with potential applications in bio-adsorbents, which highlights them for biomedical applications such as tissue engineering and drug delivery [36]

Based on the aforementioned context, the primary objectives of this research are to (1) prepare activated carbon from plastic waste char through sodium carbonate activation and citric acid modification; (2) comprehensively characterize the resulting activated carbon in terms of surface area, porosity, elemental composition, proximate analysis, and others; (3) evaluate its effectiveness in removing specific contaminants from wastewater; and (4) evaluate the economic viability and environmental sustainability of the process.

2. Materials and Methods

2.1. Preparation of Activated Carbon from Plastic Waste

The plastic waste used for this study came from the rejected fraction of a municipal solid waste facility. The composition of the plastics was determined as follows (wt. %): 55.0% polypropylene, 8.6% high-impact polystyrene, 10.1% expanded polystyrene, and 27.7% polyethylene film [44]. The material was crushed to a size smaller than 1 mm and subjected to pyrolysis in a horizontal tubular furnace (Nabertherm) under an N_2 flow of 50 L h^{-1}. The temperature increased at 10 °C/min from room temperature to a final pyrolysis temperature of 500 °C, with a holding time of 90 min. The resulting material was denoted as “char”.

The pyrolyzed char was chemically activated using Na_2CO_3 (PanReac AppliChem, Barcelona, Spain). The char was ground and mixed with the activating agent at a 1:1 mass ratio. The mixture was heated in a tubular furnace under N_2 flow (12 L h^{-1}) under the following program: heating from room temperature to 300 °C at 10 °C/min, held at 300 °C for 60 min, and then heated to 800 °C (10 °C/min) and held for 60 min. The amount of Na_2CO_3 and the activation temperature were based on previous studies [10,45]. After activation, the activated char was washed with 1 M HCl (PanReac AppliChem, Barcelona, Spain) solution (20 mL per 1 g of char), filtered, and rinsed with water until a neutral pH was achieved. The final activated material was dried at 120 °C overnight and labeled “AC”. For comparison purposes, the non-activated “char” was also washed following the same procedure.

For the citric acid (PanReac AppliChem, Barcelona, Spain) functionalization, the prepared “AC” was immersed in a citric acid solution ranging from 0.5 to 1.5 M, with a liquid-to-solid ratio of 25:4 (mL of solution per gram of activated carbon). The mixture was stirred continuously at room temperature for 30 min to ensure uniform contact between the citric acid and the activated carbon’s surface. After impregnation, the mixture was filtered and washed several times with distilled water to remove the residual citric acid. Finally, the washed activated carbon was dehydrated at 50 °C for 24 h and re-dried at 100 °C to remove moisture before storage. The resulting materials were labeled “AC-CA-X”, where X refers

to the citric acid concentration during the impregnation step (0.5–1.5 M). For comparison purposes, the non-activated char was also modified with citric acid, leading to the material denoted as "char-CA-X". Figure 1 schematizes the activation of the char to prepare AC and the functionalization with citric acid, AC-CA-X

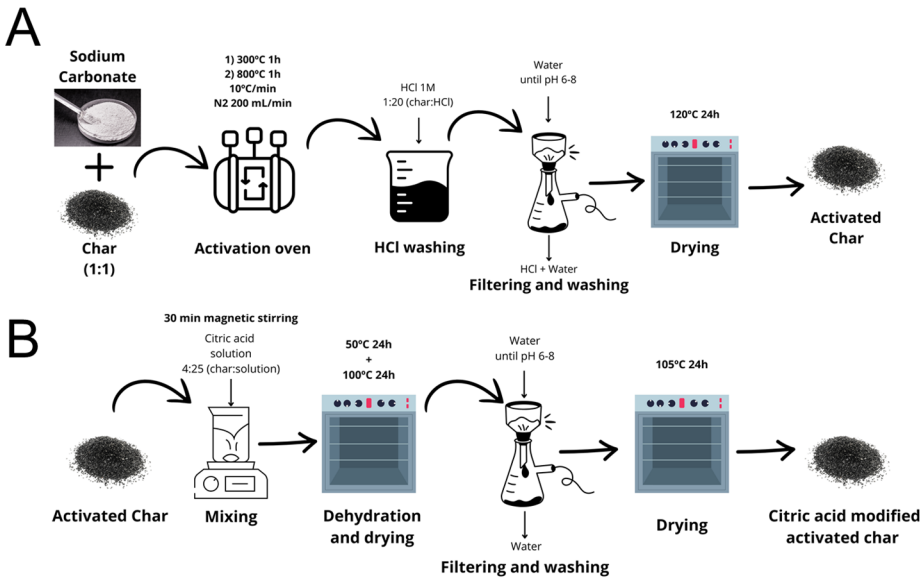

Figure 1. Activation of the char with Na_2CO_3 (**A**) and post-thermal citric acid treatment (**B**).

2.2. Characterization of Activated Carbon

The textural properties were evaluated through static gas adsorption in a Sync 200 instrument (3P Instruments®, Odelzhausen, Germany). Samples were degassed at 150 °C under vacuum for 12 h using a Prep J4 unit (3P Instruments®, Odelzhausen, Germany). The N_2 adsorption–desorption isotherms were obtained at 77 K, leading to the total surface area (S_{BET}) ascertained using the BET method. The micropore surface area (S_{MP}) and micropore volume (V_{MP}) were determined using the t-plot method. The pore size distribution was derived from CO_2 adsorption at 273 K, applying the Horvath–Kawazoe (HK) model [46,47].

The bulk chemical composition was determined by proximate and elemental analysis. Proximate analysis was performed using a Perkin Elmer® STA 6000 thermobalance (Waltham, MA, USA). Samples were heated under N_2 (20 mL min^{-1}) with the following temperature profile: held at 30 °C for 20 min, then heated to 110 °C (20 °C min^{-1}), and held for 20 min to measure moisture content. The volatile matter was determined by heating to 850 °C (20 °C min^{-1}) and holding for 20 min. Ash content was measured by switching the gas from N_2 to O_2 (20 mL min^{-1}) and maintaining it at 850 °C for 20 min. Elemental analysis (CHNS) was carried out using a Thermo Scientific™ Flash 2000 analyzer (Waltham, MA, USA). Samples were combusted at approximately 1400 °C, producing CO_2, H_2O, NO_x, and SO_2, which were separated chromatographically and detected with a thermal conductivity detector. The oxygen content was tentatively estimated by subtracting the CHNS values and ash content.

The surface chemical composition was analyzed using X-ray photoelectron spectroscopy (XPS) on a Kratos AXIS Ultra-DLD device from Jenck S.A. (Buenos Aires, Argentine), with Al Kα radiation as the X-ray source. Spectra were calibrated to the C_{1s} peak (284.6 eV) of adventitious sp^3 carbon, and peak deconvolution was performed using XPS-peak software (version 4.1) under a Shirley background correction. The chemical surface was further analyzed by thermal programmed desorption (TPD) with NH_3 on an AMI-300Lite chemisorption station from Altamira Instruments® (Pittsburgh, PA, USA) equipped with a Thermal Conductivity Detector (TCD). Briefly, 100 mg of sample was loaded and

submitted to adsorption with NH_3 (10%NH_3 in He) under 100 °C, and a temperature program from 100 °C to 1000 °C was applied.

2.3. Adsorption Experiments

Batch adsorption experiments for lead and acetaminophen were conducted at 25 °C in 100 mL Erlenmeyer flasks. Solutions containing Pb from $Pb(NO_3)_2$ (PanReac AppliChem, Barcelona, Spain) at concentrations ranging from 10 to 300 mg L^{-1} and acetaminophen (Merck®, Burlington, MA, USA) at concentrations ranging from 10 to 1000 mg L^{-1} were prepared, using an adsorbent dose of 2.0 g L^{-1}, and stirred at 160 rpm, maintaining the temperature at 25 °C until equilibrium was reached. The samples were filtered through Millipore Millex-GV PVDF 0.45 µm syringe filters, and the concentration was measured by atomic absorption spectroscopy (PerkinElmer® PinAAcle 500, Waltham, MA, USA) for Pb; high-pressure liquid chromatography (HPLC) using a Waters™ Alliance e2695 HPLC (Milford, MA, USA) with a 2998 photodiode array detector was used for the quantification of acetaminophen. A Zorbax Bonus-RP column (4.6 mm × 150 mm, 5 µm) was used as the stationary phase.

The adsorption uptake reached at equilibrium (q_e) was fitted to the two-parameter models of Langmuir (Equation (1)) and Freundlich (Equation (2)), and the three-parameter model of Sips (Equation (3)):

$$q_e = \frac{q_{max} K_L C_e}{1 + K_L C_e} \quad (1)$$

$$q_e = K_F {C_e}^{1/n_F} \quad (2)$$

$$q_e = \frac{q_{max} K_S {C_e}^{1/n_S}}{1 + K_S {C_e}^{1/n_S}} \quad (3)$$

where q_e is the amount of adsorbate per unit mass of adsorbent at equilibrium (mg g^{-1}); C_e is the equilibrium concentration of absorbate in the liquid phase (mg L^{-1}); q_{max} is the theoretical maximum adsorption capacity (mg g^{-1}); K_L is the Langmuir constant related to the affinity of the binding sites (mg^{-1} L); K_F is the Freundlich constant related to the adsorption capacity $(mg \cdot g^{-1})/(mg \cdot L^{-1})^{1/nF}$; n_F and n_S are the heterogeneity factors, indicating the intensity of adsorption (dimensionless) of the Freundlich and Sips models, respectively; and K_S is the Sips constant related to the affinity of the binding sites $(mg^{-1}\ L)^{1/ns}$.

Finally, the prepared char-based material adsorbents were also subjected to leaching tests under unmodified pH conditions to ensure the sustainability of the treatment process. The experiment involved preparing a mixture of 10 g of char with 100 mL of water, maintaining a ratio of 1:10. This mixture was agitated at a speed of 10 rpm for 24 h. Following the agitation period, the leachate was filtered using a 0.45 µm filter (PVDF Millex-HV, Merck KGaA, Darmstadt, Germany), and the released metals were quantified by Induced Coupled Plasma-Mass Spectrometry (ICP-MS) in a Perkin Elmer Nexion 300D device (Waltham, MA, USA).

2.4. Environmental Assessment

For the environmental assessment, the life cycle analysis (LCA) methodology was applied. The standards that define the LCA methodology are the Standard "UNE-EN ISO 14040:2006. Environmental management. Life cycle analysis. Principles and reference framework" [48] and "Standard UNE-EN ISO 14044:2006/A1:2018. Environmental management. Life cycle assessment. Requirements and guidelines" [49]. In this study, the SimaPro 9.4.0.1 PhD software (PRé Sustainability B.V.) and the ReCiPe 2016 method were employed for the process modeling and assessing environmental impacts.

3. Results and Discussion

3.1. Characterization of the Char-Based Materials

Table 1 summarizes the effect of Na_2CO_3 activation and citric acid modification at different dosages on the key properties of the char materials, including surface area, microporosity, and CO_2 adsorption capacity at 100 kPa. The untreated char displays a low specific surface, no microporosity, and null CO_2 adsorption, while the char submitted to activation with Na_2CO_3, without citric acid modification, shows the highest specific surface area (S_{BET} = 417.6 m^2 g^{-1}) and a significant micropore contribution (S_{MP} = 247.2 m^2 g^{-1}, V_{MP}/V_T = 28.9%). This material also led to the highest CO_2 adsorption capacity (q_{CO2} = 73.7 mg g^{-1}), suggesting that Na_2CO_3 activation alone significantly enhances the char's adsorption capacity. As reported in the activation of other plastics such as polyacrylonitrile, the thermal decomposition of Na_2CO_3 can develop porosity in the structure [50]. However, as observed in the N_2 isotherms illustrated in Figure 2A, a type IV isotherm was observed according to the IUPAC guidelines [51], with an important rise at low pressures, which suggests that the material compromises a mixed contribution of mesopores and micropores.

Table 1. Textural properties after Na_2CO_3 activation and citric acid modification by N_2 adsorption isotherms at 77 K and CO_2 adsorption at 273 K.

Sample	S_{BET} (m^2 g^{-1})	S_{MP} (m^2 g^{-1})	V_T (cm^3 g^{-1})	V_{MP} (cm^3 g^{-1})	V_{MP}/V_T (%)	q_{CO2} at 100 kPa (mg g^{-1})
char	2.6	0.0	0.009	0.000	0.0	16.8
char-CA-1.0	19.4	0.0	0.074	0.000	0.0	22.1
AC	417.6	247.2	0.436	0.126	28.9	73.8
AC-CA-0.5	324.9	175.5	0.371	0.093	25.1	57.5
AC-CA-1.0	341.0	141.6	0.424	0.072	16.9	55.0
AC-CA-1.5	356.4	186.0	0.392	0.098	25.0	59.3

S_{BET}: total specific surface area by BET method; S_{MP}: micropore surface area by t-plot method; V_T: total pore volume from N_2 uptake at p/p_0~0.99; V_{MP}: micropore volume by t-plot method; q_{CO2}: CO_2 uptake at 100 kPa and 273 K.

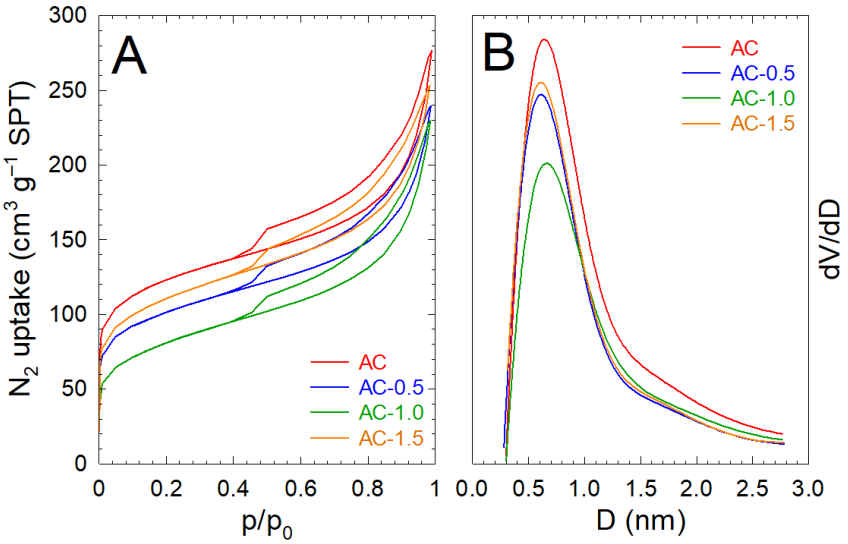

Figure 2. N_2 adsorption–desorption isotherms at 77 K (**A**) and micropore size distribution (**B**) by the HK method obtained from the CO_2 adsorption isotherm at 273 K of the activated carbon after citric acid modification.

The char modified with CA 1 M led to a minimal rise in the textural properties, S_{BET} = 19.4 m^2 g^{-1}, and V_T = 0.074 cm^3 g^{-1}, probably due to the reaction of labile carbon

during the acid treatment. However, microporosity was completely absent both in the char before and after CA modification. The CA treatment of the activated char with Na_2CO_3 produced a decrease in the total surface area and pore volume in all cases. The surface interactions of CA with the original AC display the occlusion of micropores and partial reaction with the most reactive surface groups, indicating lower micropore contribution with lower V_{MP}/V_T ratios. Similar findings have been reported during the CA modification of commercial activated carbon formulas, in which 34% of the surface area was registered [52]. From all the CA-modified samples, the AC-CA-1.0 outlines the highest mesoporosity reached after CA treatment, and consequently the lowest CO_2 uptake due to the preferred microporosity contribution required by the adsorption of this molecule. Regarding the micropore size distribution, due to the use of Na_2CO_3 as an activating agent, the micropore size contribution registered in Figure 2B is addressed at 0.6–0.7 nm due to the CO_2 released during the thermal decomposition of Na_2CO_3 [53].

The proximate analysis was used as a tool to predict the carbon content in all the samples, leading to the results presented in Table 2. The non-activated and untreated char exhibits relatively low moisture (2.9%) and high ash content (38.8%), highlighting a significant inorganic presence; the fixed carbon content remains as low as 28.3%, suggesting limited carbon retention, to the detriment of volatile matter (30.0%). After activation with Na_2CO_3, the volatile matter content decreased and the ash content increased, an effect ascribed to the concentration of inorganic matter. The CA modification of the char increased the fixed carbon percentage, demonstrating the anchorage of CA molecules onto the surface. Following the CA functionalization of the activated char, a certain balance emerges. For instance, with 0.5 M citric acid, the fixed carbon remains high at 33.6%, while the ash content is somewhat controlled at 46.3%. At a higher CA concentration, i.e., 1.5 M citric acid, the fixed carbon declines slightly to 31.3%, and the ash content increases to 48.5%. This phenomenon suggests that the combination of Na_2CO_3 activation and CA post-treatment enhances the contribution of carbon, and the citric acid concentration must be carefully optimized to balance carbon fixation and ash minimization.

Table 2. Proximate and elemental analysis (wt. %) after Na_2CO_3 activation and citric acid modification.

Sample	Proximate Analysis				Elemental Analysis *			
	Moisture	Volatile	Fixed Carbon	Ash	C_{EA}	H_{EA}	N_{EA}	O_{EA}
Char	2.9	30.0	28.3	38.8	37.0	2.4	1.0	20.8
char-CA-1.0	3.2	16.1	36.8	43.9	44.3	2.0	1.8	8.0
AC	8.6	9.4	20.9	61.1	32.8	1.3	0.7	4.4
AC-CA-0.5	8.8	11.3	33.6	46.3	39.1	1.3	0.9	12.4
AC-CA-1.0	7.9	12.4	32.4	47.3	39.4	1.3	0.8	11.2
AC-CA-1.5	7.4	12.8	31.3	48.5	39.7	1.1	0.9	9.8

* No S was detected in any sample. The O is estimated as the difference after ashes subtraction.

The carbon content in the bulk of the samples was estimated by elemental analysis, as shown in Table 2. All the samples exhibited moderate carbon content. The char exhibited 37.0%, whereas the activation with Na_2CO_3 decreased the value to 32.8%, which is commonly observed during chemical activation with a wide range of different reagents [54]. The combination of a strong oxidizing medium and dehydrating effects justifies this increase in the C content [55]. The citric acid modification increased the carbon content either in the non-activated char or in that activated with Na_2CO_3. Concretely, the CA modification of the non-activated char led to the highest carbon content, e.g., 44.3%, whereas the CA-modified activated carbon displayed ~39% C. The CA functionalization of activated carbon has been

reported to increase the C content [56] due to the anchorage of CA leaving the formation of C=O species [57]. The H content remained relatively stable among all the samples but tended to slightly increase after CA treatment. The N content slightly decreased after Na_2CO_3 activation, possibly due to chemical reactions that eliminate nitrogen-containing compounds during the activation step [58]. The O contribution was estimated by the difference after ash removal. The activation with Na_2CO_3 leads to a paramount decrease in O, i.e., from 20.8% (char) to 4.4% (AC), due to the reaction of Na_2CO_3 with the oxygenated groups on the surface of the char and the associated dehydration reactions. The CA post-treatment in the CA post-treated AC samples raised the O content, probably due to the cross-linking effect of CA.

The surface composition was analyzed by the XPS technique. The quantification results are shown in Table 3. Different trends regarding the surface carbon content (C_{XPS}) were observed compared to the bulk percentages reported by elemental analysis. However, C_{XPS} also decreased after activation with Na_2CO_3, and the samples functionalized with CA also displayed a growth in C_{XPS} content. The O_{XPS} content should be taken under caution since the presence of oxygenated metals hinders the calculation of the specific O content linked to the carbonaceous matrix. Furthermore, the presence of some metals was registered, specifically Si and Ti, which are commonly dosed in plastic polymers as additives. Silica, silicon dioxide, and $CaCO_3$ are commonly added as reinforcing fillers while Ti is dosed as TiO_2 due to its whiteness and brightness to modify the color of the final polymeric product [59]. The surface contents of these inorganic components increase from the char to the char-CA and the AC-CA-X samples as they are concentrated in the solid. In addition, the nature of the chemical bonding of C and O was assessed by the deconvolution of C_{1s} and O_{1s} spectra. The high-resolution C_{1s} spectrum was interpreted by the deconvolution of the following contributions: sp^2 C=C (284.6 eV), sp^3 C-C (285.3 eV), C-O (286.6 eV), C=O (288.0 eV), and O=C-O-R (289.9 eV) [60,61]. As an example, Figure 3 illustrates the deconvolution for the samples char, AC, and AC-CA-1.0. The contributions of each of the samples are available in Table 3 and depicted in Figure 3. The process of activation increases the percentage of sp^2 carbon to the detriment of sp^3, probably due to the thermal dehydration reactions during the Na_2CO_3 activation. The CA modification of the AC led to a decrease in the sp^2 C=C bonds and positively impacted the formation of oxygenated groups, especially C=O and C-O. Concretely, if the percentage of oxygenated carbon is accounted for (Sum C_{ox}), the performance of the materials is described in the following order: char (4.5%) < char-CA-1.0 (17.2%) < AC (15.6%) < AC-CA-0.5 (18.0%) < AC-CA-1.0 (30.1%) < AC-CA-1.5 (24.0%). Hence, a positive effect from the activation with Na_2CO_3 is deduced, especially with CA functionalization to enhance the presence of oxygenated carbonaceous groups. The activated and modified AC-CA-1.0 displays the highest value, i.e., double the value of the unmodified AC sample. In this sample, although all the oxygenated contributions were raised, the C-O outweighed the rest. The high-resolution O_{1s} region was adjusted into three plausible contributions, i.e., quinone (530.7 eV), C=O (531.5–532.0 eV), and C-O (~533 eV) [62]. From the evolution of their relative contributions, we ascertained a rise in C=O to the detriment of the quinone groups as the samples were treated with CA, with the AC-CA-1.0 being the sample in which this effect is most noticeable.

The nature of the oxygenated groups was further qualitatively evaluated by TPD. The TPD profiles are depicted in Figure 4. A tentative deconvolution was conducted based on the temperature at which the oxygenated functional groups decompose. According to the literature [63], carboxylic acids decompose below 400 °C, carboxylic anhydrides decompose between 350 and 600 °C, and lactones reveal a peak above 600 °C. Phenol groups are registered in a middle-temperature range of 500–750 °C, while carbonyl/quinone groups

release CO above 700 °C. Finally, pyrone-like groups, if present, are released at 950 °C. On this basis, the TPD profiles were deconvoluted. The char showed the lowest release of TCD signal, attributable to low oxygenated species on the surface. After CA treatment of the char, the TCD signal rose, as a consequence of the oxygenated groups increasing. The activation of the char with Na_2CO_3 led to a material with the presence of carboxyl groups, phenol, and carbonyl groups resistant to thermal treatment, close to pyrone behavior. The CA post-thermal modification enriched the variety of carbonyl and quinone groups, with contributions at lower temperatures compared to the non-modified AC. Interestingly, the TPD profiles confirm that the modification with CA destroyed the presence of carboxyl groups as the concentration of CA increased. From the profiles attained, it can be concluded that the modification with CA enriched the variety of contributions ascribed to the range of release of carbonyl and quinone, mainly.

Table 3. XPS surface chemical composition and C_{1s} contribution after Na_2CO_3 activation and citric acid modification.

Sample	Surface Composition (wt. %)				C_{1s}		O_{1s}	
	C_{XPS}	O_{XPS}	N_{XPS}	Others	Type	Peak (%)	Type	Peak (%)
char	86.4	10.8	0.7	1.3 (Si) 0.8 (Ti)	C=C C-C C-O C=O COO- Sum C_{Ox}	44.7 42.7 4.5 - - 4.5	Quinone C=O C-O	37.6 34.2 28.3
char-CA-1.0	71.1	18.7	1.9	3.5 (Si) 3.5 (Ti)	C=C C-C C-O C=O COO- Sum C_{Ox}	65.6 17.2 2.9 8.1 6.2 17.2	Quinone C=O C-O	32.6 43.4 24.0
AC	32.2	38.6	1.0	10.8 (Si) 11.0 (Ti) 2.1 (P) 2.1 (Ca) 1.9 (Fe)	C=C C-C C-O C=O COO- Sum C_{Ox}	68.2 16.2 - 10.5 5.1 15.6	Quinone C=O C-O	35.5 40.3 24.2
AC-CA-0.5	49.3	32.3	1.0	9.9 (Si) 5.1 (Ti) 1.1 (P)	C=C C-C C-O C=O COO- Sum C_{Ox}	59.9 22.1 2.4 10.5 5.1 18.0	Quinone C=O C-O	28.4 42.3 29.2
AC-CA-1.0	47.7	33.0	1.3	11.0 (Si) 4.2 (Ti) 1.3 (P)	C=C C-C C-O C=O COO- Sum C_{Ox}	44.6 25.3 17.2 8.3 4.6 30.1	Quinone C=O C-O	28.0 49.5 22.5
AC-CA-1.5	49.9	30.8	1.3	10.8 (Si) 4.6 (Ti) 1.2 (P)	C=C C-C C-O C=O COO- Sum C_{Ox}	60.5 15.4 9.7 5.9 8.4 24.0	Quinone C=O C-O	24.4 45.9 29.7

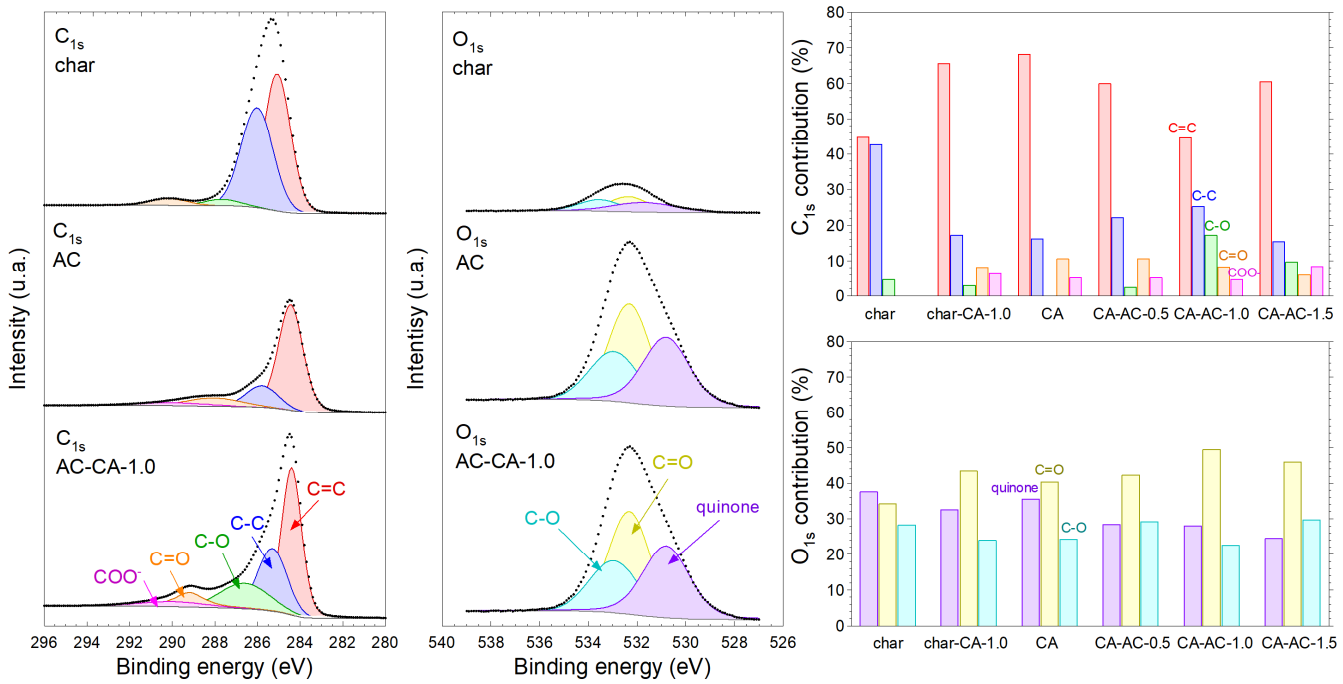

Figure 3. High-resolution XPS spectra of C_{1s} (**left**) and O_{1s} (**middle**) regions for char, AC, and AC-CA-1.0, and the deconvoluted contribution for all the samples (**right**).

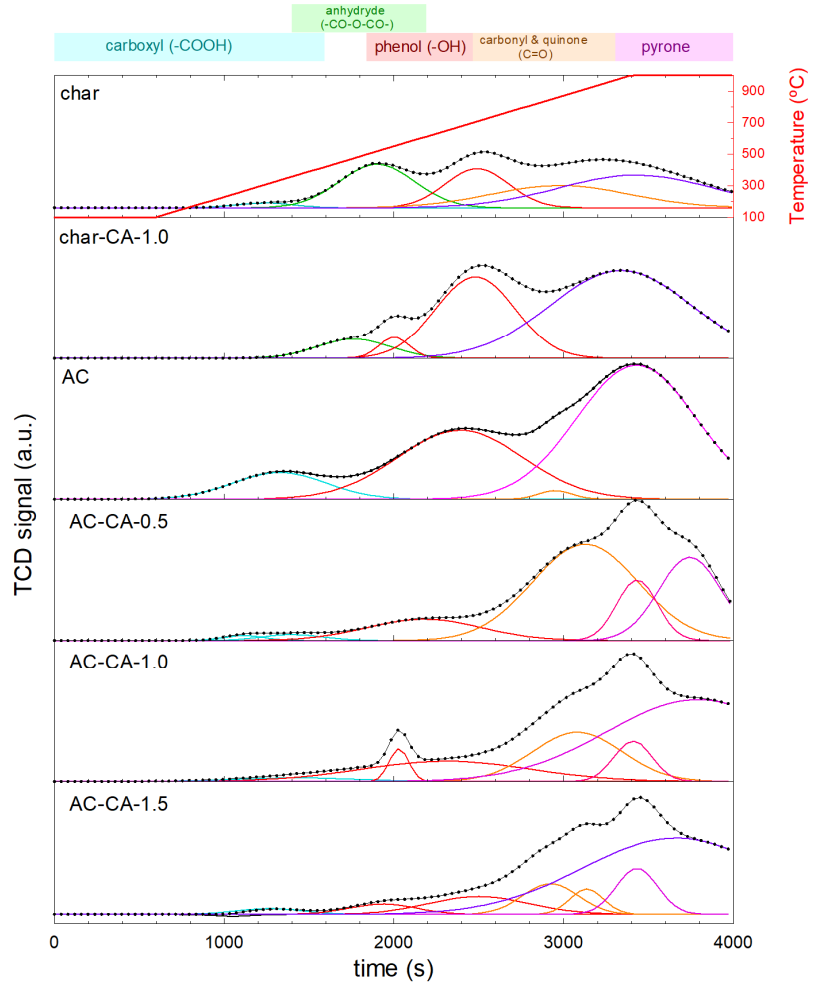

Figure 4. TPD profiles of the char and the activated carbon after citric acid modification.

3.2. Adsorption of Lead and Acetaminophen

The modification of the activated carbon with CA was first studied on the adsorption of lead in water, a metal whose occurrence remains a problem in drinking water at the ppb level [64]. The performance of each sample is illustrated with the isotherms in Figure 5. From the isotherm, it is possible to define the maximum adsorption capacity (q_{max}) for each material, as shown in Table 4. The isotherms were fitted to common models such as Langmuir, Freundlich, and Sips. The Langmuir isotherm is an empirical model that assumes monolayer formation, with homogeneous sites on the surface, and all the adsorbent sites display equal affinity towards the adsorbate, with no adsorbate transmigration in the surface plane [65]. In contrast, the Freundlich model considers the plausible formation of a multilayer and the heterogeneity of the absorbent surface [66]. The Sips model emerges as a combination of the former two, considering the heterogeneity of the adsorption systems as well as circumventing the limitations associated with the high concentration registered by the adsorbate under the Freundlich model [67]. The three-parameter Sips model was selected as the best due to a better definition of the initial increase and the plateau at high concentration. The better fitting provides insights into the plausible mechanism in which a low concentration may promote the formation of multilayers due to considerable heterogeneity, and when the activated sites are saturated, no extra adsorption takes place, reaching the characteristic plateau of the Langmuir model. The results show notable variations in the q_{max} values based on the treatment conditions, underscoring their significant influence on the char's adsorption potential. The untreated char exhibits a low value, i.e., q_{max} = 3.1 mg g^{-1}, indicating minimal adsorption capacity. However, after activation with Na_2CO_3, the CA solid displayed a higher uptake, q_{max} = 37.2 mg g^{-1}. This significant enhancement can be attributed to the improved surface area and a higher presence of surface oxygenated groups linked to the carbon matrix, facilitating better adsorption thanks to their interactions with lead-hydrated ions.

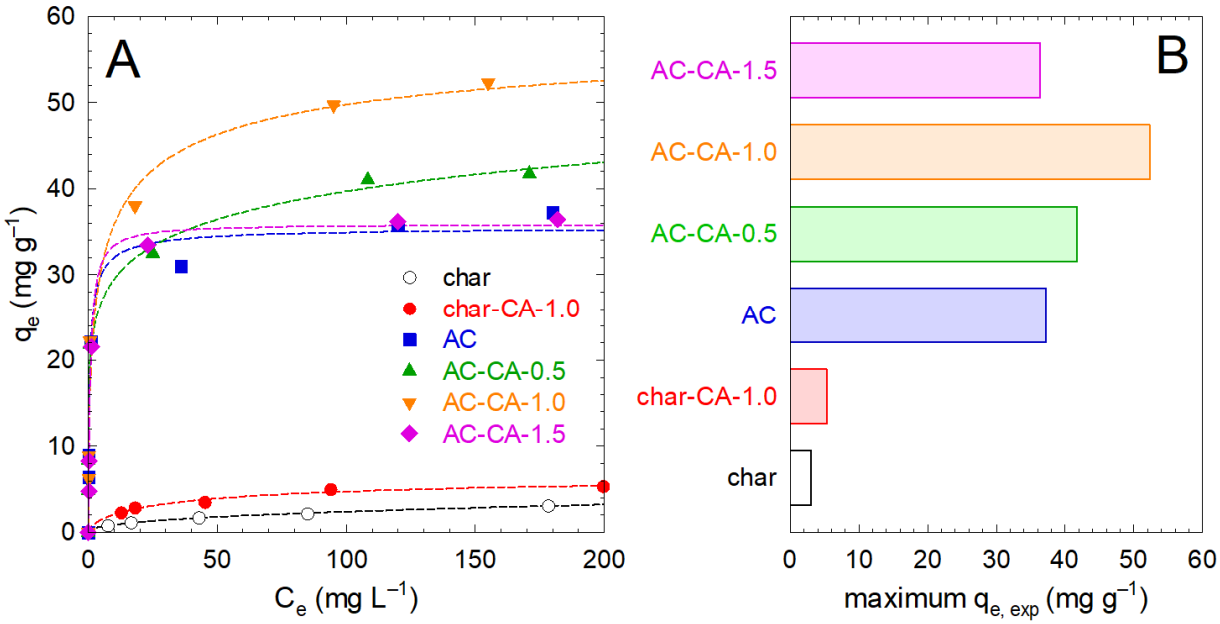

Figure 5. (**A**) Adsorption isotherms of lead with char and the activated carbon after citric acid modification. The dashed lines correspond to the Sips modeling. (**B**) Maximum experimental uptake of lead registered.

Table 4. Model fitting parameters of lead isotherm onto the char and the activated carbon after citric acid modification.

Model	Parameter	Char	char-CA-1.0	AC	AC-CA-0.5	AC-CA-1.0	AC-CA-1.5
Langmuir	q_{max}	3.59	5.86	34.67	38.74	48.04	35.93
	K_L	0.02	0.05	2.36	2.36	1.08	1.32
	R^2	0.959	0.952	0.979	0.953	0.948	0.995
Freundlich	K_F	0.34	1.22	16.34	20.44	17.94	15.71
	n_F	2.35	3.48	6.05	6.94	4.52	5.64
	R^2	0.999	0.944	0.907	0.947	0.932	0.874
Sips	q_{max}	5.00	7.22	35.66	50.0	60.81	35.93
	K_S	0.04	0.09	1.60	0.85	0.46	1.32
	n_S	1.46	1.49	1.35	3.17	2.01	1.00
	R^2	0.985	0.964	0.981	0.945	0.955	0.995

q_{max}, theoretical maximum adsorption capacity (mg/L); K_L, Langmuir constant (L/mg); K_F, Freundlich constant; n_S is the heterogeneity factor of Sips model (dimensionless); and K_S, is the Sips constant.

In the case of the char modified with CA, the q_{max} rises slightly to 5.3 mg g^{-1}, revealing the limited effectiveness of the functionalization on the non-activated char. In contrast, the CA functionalization of the activated samples boosts the metal adsorption uptake. Specifically, the values obtained were 41.7 mg g^{-1} (AC-CA-0.5), 52.3 mg g^{-1} (AC-CA-1.0), and 36.4 mg g^{-1} (AC-CA-1.5). This performance matches the contribution of oxygenated carbon as deduced with XPS, with the sample AC-CA-1.0 being the most enriched. Thus, there exists an optimal range for citric acid concentration, which leads to an enhanced contribution of oxygenated groups in the carbon matrix that triggers the maximum lead adsorption efficiency. Therefore, an optimum functionalization of the carbon material maximizes the capacity to retain metal, which is crucial for applications in environmental remediation. Comparative studies have reported similar results for Na_2CO_3-activated carbon derived from other feedstocks. For example, the activation of rapeseed oil cake with Na_2CO_3 improves the adsorption capacity for lead ions if compared to the non-activated material, achieving a maximum lead uptake of q_{max} = 130 mg g^{-1}, indicating the effectiveness of this activating agent [68]. Additionally, the maximum adsorption capacity for lead ions using Na_2CO_3-activated carbon prepared from *Cedrus deodara* bark was reported to be 236.4 mg g^{-1} [32]. In a study focused on activated carbon prepared from rice husk and treated with 5% Na_2CO_3, the lead adsorption capacity was approximately 0.6 mg g^{-1} [23]. Furthermore, the modification of citric acid enhances the adsorption uptake of lead to q_{max} = 41.7 mg g^{-1} [69].

Citric acid functionalization was also assessed for the adsorption of a representative contaminant of emerging concern, such as acetaminophen [70,71]. Figure 6 portrays the acetaminophen isotherms, and Table 5 summarizes the results achieved for fitting with the most common adsorption models, with the Sips model generally providing the best fit for the experimental data. The untreated char exhibits a relatively low acetaminophen uptake, experimentally around 10 mg g^{-1}, indicating a poor adsorption performance. In contrast, the activated carbon boosts the maximum q_{max} to ca. 80 mg g^{-1}, showcasing the effectiveness of this activation method in creating a more porous structure with a higher surface area, which facilitates better acetaminophen adsorption. The citric acid modification did not substantially alter the acetaminophen efficiency, with a similar maximum experimental adsorption capacity observed. This suggests that citric acid alone does not enhance, and may even hinder, the char's ability to adsorb acetaminophen. Nevertheless, when combined with Na_2CO_3 activation, the adsorption uptake is enhanced to a value of roughly 80 mg g^{-1}. The modification of the activated material with citric acid did not improve the

adsorption uptake compared to the non-modified sample. This evidence suggests that the mechanism of acetaminophen adsorption does not require the presence of carboxylic acid, which, according to the XPS characterization, is the prime oxygenated group after citric acid functionalization. The literature reports very different adsorption uptakes, strongly affected by the chemical activating agent used and the nature of the carbonaceous precursor material. For example, the activation of Brazil nutshell with $ZnCl_2$ can create an adsorbent with an uptake as high as 285 mg g^{-1} [72]. The activation of spent tea leaves with H_3PO_4 only retains about 59 mg L^{-1} [73]. Or, in the case of the activation of rice with NaOH only, the acetaminophen removal rate is 50 mg g^{-1} [74]. Regarding the role played by citric acid in similar carbonaceous materials, the activation of materials from citrus waste with $FeCl_3$ only reached an acetaminophen yield of 45 mg g^{-1} [75].

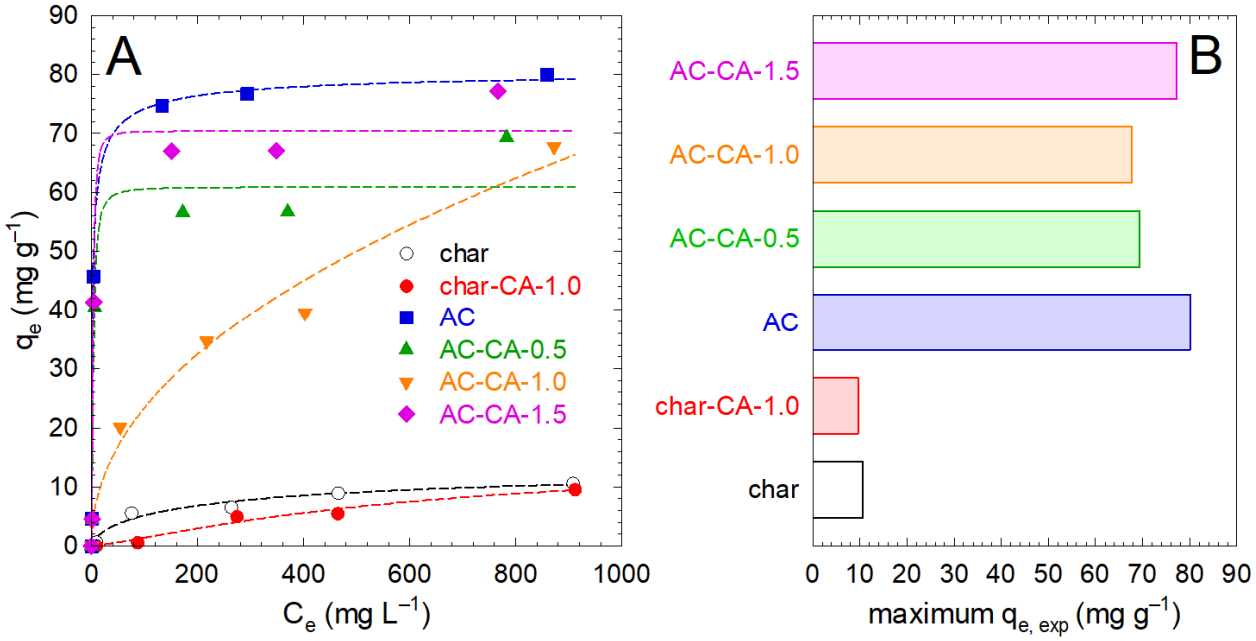

Figure 6. (**A**) Adsorption isotherms of acetaminophen with char and the activated carbon after citric acid modification. The dashed lines correspond to the Sips modeling. (**B**) Maximum experimental uptake of acetaminophen registered.

Table 5. Model fitting parameters of acetaminophen isotherm onto the char and the activated carbon after citric acid modification.

Model	Parameter	Char	char-CA-1.0	AC	AC-CA-0.5	AC-CA-1.0	AC-CA-1.5
Langmuir	q_{max}	11.07	23.26	77.77	62.00	90.77	71.66
	K_L	0.01	0.00	0.53	0.27	0.00	0.29
	R^2	0.943	0.970	0.997	0.951	0.947	0.968
Freundlich	K_F	0.91	0.05	33.09	20.16	2.67	22.91
	n_F	2.73	1.31	6.93	5.36	2.12	5.27
	R^2	0.941	0.964	0.917	0.844	0.979	0.858
Sips	q_{max}	14.87	7.28	81.27	60.97	100.00	70.46
	K_S	0.02	0.01	0.71	0.15	0.01	0.15
	n_S	1.50	1.76	1.71	0.67	1.31	0.57
	R^2	0.957	0.942	1.000	0.958	0.949	0.980

3.3. Stability of the Material: Leachates Analysis

The stability of the prepared carbonaceous adsorbent was examined and aimed at the analysis of the plausible metals released in an aqueous solution. Table 6 summarizes

the concentrations of the major and minor metallic elements of a selection of the materials prepared, i.e., char, char-CA-1.0, AC, and AC-CA-1.0. The leachate analysis revealed that the activation with Na_2CO_3, and the further modification with citric acid, significantly alters the concentration of the released species in the solution. Na_2CO_3 generally increases the levels of major elements like Ca and P, detected on the surface by the XPS technique. The citric acid treatment influences minor elements such as Cd, Co, and Sb. The sequential activation with Na_2CO_3 and citric acid functionalization tends to maximize the concentration of several components, especially Ti and Sb. The findings suggest that using plastic residues as precursors for the preparation of activated carbon requires a detailed investigation of the leaching of metallic impurities incorporated in the polymeric structure of this residue as an additive [59]. The components that are lixiviated to a larger extent, such as Ca, P, Si, and Ti, do not display any problems for environmental applications in water due to the lack of toxicity. In contrast, the metals that might compromise the toxicity of the released effluent were detected at low concentrations, bearing in mind that the presented data in Table 6 correspond to a solid–water (m/v) ratio of 1:10, an abnormally high dosage.

Table 6. Leached metals into aqueous solution by selected samples. Solid-to-water ratio (m/v) 1:10.

Elements		Char	char-CA-1.0	AC	AC-CA-1.0
Major elements (mg L^{-1})	Al	0.95	0.60	0.03	3.08
	Ca	44.2	3.04	83.88	16.44
	Fe	0.03	0.54	<0.01	4.12
	K	0.18	0.97	0.59	3.34
	Mg	12.19	1.05	19.46	4.73
	Na	0.08	5.46	<0.01	22.57
	P	11.49	0.41	122.50	3.49
	S	1.50	1.91	5.60	19.05
	Si	11.18	1.28	53.16	38.97
	Zn	1.18	1.97	>0.01	0.657
Minor elements (µg L^{-1})	As	2.6	6.6	0.6	4.2
	Ba	739.5	401.9	2.4	217.3
	Cd	1.8	65.0	0.9	10.2
	Co	10.2	134.3	19.9	18.3
	Cr	12.0	64.7	3.6	111.0
	Cu	116.5	37.6	91.8	213.1
	Ga	18.9	20.4	0.1	11.0
	Li	28.1	43.6	25.5	10.7
	Mn	91.6	115.1	10.7	114.9
	Mo	0.1	82.3	0.2	77.9
	Ni	116.5	156.3	91.8	67.7
	Pb	140.1	4.1	12.4	1.2
	Rb	13.4	16.0	8.0	13.7
	Sb	0.4	470.4	0.0	2587.4
	Se	3.3	4.1	5.4	1.5
	Sr	311.9	255.5	22.5	108.6
	Ti	2.5	194.0	45.0	2448.1
	V	2.5	4.1	21.7	4.0

3.4. Economic and Environmental Assessment

An economical pre-evaluation was tentatively conducted to evaluate the role of the activation process and citric acid modification on the adsorption efficiency. Table 7 summarizes the costs associated with the adsorption of lead and acetaminophen using char materials, expressed as EUR per kilogram of the contaminants retained, and the preparation cost of each analyzed material. The yield during the synthesis, as shown in Table 7,

was accounted for in the cost estimation. Briefly, the activation with Na_2CO_3 led to a 31.7% yield and the post-treatment with citric acid did not substantially alter this value. The untreated char shows moderate adsorption costs for both lead (2214.0 EUR/kg) and acetaminophen (1046.3 EUR/kg). In contrast, the application of Na_2CO_3 activation reduced these costs, with lead adsorption costs dropping to 1169.7 EUR/kg and acetaminophen to 582.4 EUR/kg. This cost reduction is the consequence of the enhanced adsorption capacity achieved after activation, making the process more economically viable for both contaminants. The citric acid modification of the non-activated char increased the costs of lead (5008.9 EUR/kg) and acetaminophen (5029.0 EUR/kg) removal. This suggests that citric acid alone may hinder the adsorption efficiency, leading to higher costs per unit of contaminant retained. Conversely, with the citric acid functionalization of the activated char at low CA dosage (0.5 M), the costs decrease to 1506.8 EUR/kg for lead and 906.9 EUR/kg for acetaminophen, demonstrating that a strategic combination of treatments can enhance the adsorption efficiency while maintaining low costs. At high citric acid concentration (1.5 M), the costs rise, especially for lead adsorption (2493.9 EUR/kg), indicating that excessive citric acid modification diminishes economic feasibility for certain applications. In addition, the preparation costs of each material vary between 4.7 and 25.1 EUR/kg. Although the results found are a preliminary estimation based on laboratory-scale consumption and do not include some aspects to be considered at a large scale, they are like those found by other researchers. The cost of chemical activation strongly depends on the carbonaceous precursor and the activation agent, ranging within values between 8.60 USD/kg (≈7.9 EUR/kg) and 2.33 USD/kg (≈2.1 EUR/kg) [76]. In conclusion, while Na_2CO_3 activation significantly enhances performance and reduces costs, careful consideration of citric acid concentrations is necessary to maintain economic viability. These findings indicate that the development of optimized adsorbent materials can lead to effective and affordable solutions for environmental remediation, making them attractive options for treating hazardous contaminants like heavy metals and organic anthropogenic pollutants of emerging concern.

Table 7. Effects of activation and citric acid modification on preparation and treatment costs.

Sample	Yield (%)	Preparation Costs (EUR/kg Material) [1]	Lead Removal Costs (EUR/kg) [2]	Acetaminophen Removal Costs (EUR/kg) [2]
Char	-	4.7	2214.0	1046.3
char-CA-1.0	67.7	14.9	5008.9	5029.0
AC	31.7	13.8	1169.7	582.4
AC-CA-0.5	31.1	17.5	1506.8	906.9
AC-CA-1.0	31.4	21.3	1714.5	1258.1
AC-CA-1.5	30.9	25.1	2493.9	1172.5

[1] Preparation costs per kg of material prepared; [2] material costs associated with the treatment per kg of contaminant removed.

The environmental impact of the four char preparation methods was estimated, considering not only the adsorption efficiency but also the environmental performance under different scenarios. The environmental impact assessment was undertaken following a streamlined life cycle assessment (LCA) methodology. LCA is widely used to determine the environmental impact of processes, considering upstream and downstream emissions and the resources consumed. Four plausible scenarios were modeled based on the treatment of 1 g of char, i.e., the functional unit defined for this study. The inputs and outputs employed to build the data inventory include the reagents consumed, heating, and emissions to water, as shown in Table S1. The upstream and downstream emissions and use of resources were collated from the commercial database ecoinvent 3.10 using the allocation, cut-off by the

classification system model. The software SimaPro 9.6.0.1 was applied to manage the data and perform life cycle calculations. The comparative results are presented in Figure 7.

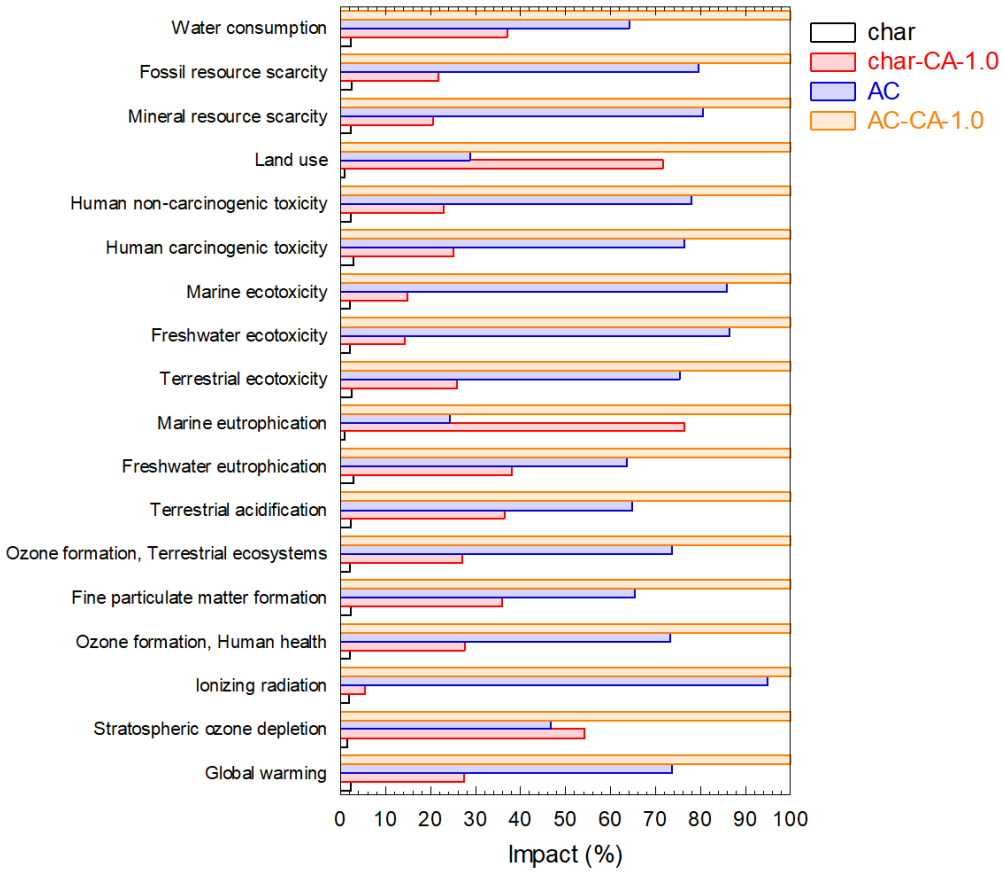

Figure 7. Environmental impact comparison of the four scenarios.

The results depicted in Figure 7 demonstrate that the scenarios involving citric acid utilization have an environmental impact that is markedly higher than that observed in scenarios that do not employ citric acid. This conclusion applies to all environmental impact categories. Overall, the environmental impact of washing and modifying the char with citric acid is 12 times higher than that of washing alone. Additionally, the environmental impact of washing, activating, and modifying the char with citric acid is 1.4 times higher than just the activated char. For all environmental impact categories, the scenario exhibiting the highest impact is one including washing, activation, and functionalization with citric acid. Furthermore, the process of activation makes a considerable contribution to the overall environmental impact. In all scenarios, the most significant contributor to the overall environmental impact is human carcinogenic toxicity, followed by freshwater and marine ecotoxicity. This is largely attributable to the high energy requirements of the drying processes. In conclusion, although modifying the char with citric acid may enhance the adsorption performance, it also considerably increases the environmental impact. Therefore, citric acid usage leads to enhanced adsorption uptake and minimizes the preparation and removal costs; however, its use results in detrimental consequences from an environmental point of view [77–79].

4. Conclusions

Plastic waste that is no longer suitable for mechanical recycling due to a lack of quality or to the complexity of a mixed composition can be successfully transformed via pyrolysis and chemical activation into activated carbon, with potential environmental applications

as an adsorbent. Activation with sodium carbonate triggers the formation of mesoporous activated carbon, i.e., non-porous char ~3 m^2 g^{-1} vs. the activated char ~418 m^2 g^{-1} and pore volume 0.436 cm^3 g^{-1} with 71% mesopores contribution. The surface oxygenated groups can be enriched with a post-treatment process involving citric acid impregnation. Although a partial surface loss is observed due to a partial blockage of the cross-linked citric acid, the presence of carbonyl and carboxyl groups is considerably boosted. The oxygen-enriched terminal carbonaceous groups were relevant in the adsorption uptake of lead in water, raising the maximum lead uptake from water ~37 mg g^{-1} (activated carbon) to ~52 mg g^{-1} (activated material after citric acid functionalization). In the case of acetaminophen adsorption, the citric acid did not show any substantial improvement concerning the activated material (80 mg g^{-1} acetaminophen uptake). The higher efficiency of the activated and citric acid-treated adsorbents minimizes the material required, but these materials are employed at a higher cost. Nevertheless, the environmental impact associated with activation steps, citric acid modification, and washing of the material negatively impacts the released emissions. According to a life cycle assessment, sodium carbonate activation strongly increases the impacts compared to the additional environmental costs of citric acid functionalization.

Supplementary Materials: The following supporting information can be downloaded at https://www.mdpi.com/article/10.3390/app15031634/s1, Table S1: Inputs and outputs of the inventory. Data calculated per 1 g of treated char.

Author Contributions: Conceptualization, L.P.; Data curation, L.P.; Formal analysis, L.P., M.Á.M.-L., C.C. and T.R.; Funding acquisition, M.Á.M.-L. and M.C.; Investigation, L.P., M.Á.M.-L. and R.R.S.; Methodology, L.P.; Project administration, M.Á.M.-L. and M.C.; Resources, M.C.; Software, G.G.-G.; Supervision, M.Á.M.-L. and R.R.S.; Validation, R.R.S.; Visualization, L.P.; Writing—original draft, M.Á.M.-L. and R.R.S.; Writing—review and editing, G.G.-G., C.C., T.R. and M.C. All authors have read and agreed to the published version of the manuscript.

Funding: This research was funded by the Ministry of Science and Innovation and the Research State Agency (10.13039/501100011033) and the European Union Next Generation EU/PRTR, Projects Oriented to Ecological and Digital Transition 2021, grant number TED2021–130157B-I00. Guillermo Garcia-Garcia acknowledges the Grant 'Marie Skłodowska-Curie Actions (MSCA) Postdoctoral Fellowship' with Grant agreement ID: 101052284.

Data Availability Statement: The raw data supporting the conclusions of this article will be made available by the authors upon request.

Acknowledgments: The authors are grateful for the support provided by the external services of investigation of the University of Granada (*Centro de Instrumentación Científica*, CIC).

Conflicts of Interest: The authors declare no conflicts of interest.

References

1. Abila, B.; Kantola, J. Waste Management: Relevance to Environmental Sustainability. *Int. J. Environ. Waste Manag.* **2019**, *23*, 337–351. [CrossRef]
2. Kibria, M.G.; Masuk, N.I.; Safayet, R.; Nguyen, H.Q.; Mourshed, M. Plastic Waste: Challenges and Opportunities to Mitigate Pollution and Effective Management. *Int. J. Environ. Res.* **2023**, *17*, 20. [CrossRef]
3. Williams, A.T.; Rangel-Buitrago, N. The Past, Present, and Future of Plastic Pollution. *Mar. Pollut. Bull.* **2022**, *176*, 113429. [CrossRef] [PubMed]
4. Yuan, Z.; Nag, R.; Cummins, E. Human Health Concerns Regarding Microplastics in the Aquatic Environment—From Marine to Food Systems. *Sci. Total Environ.* **2022**, *823*, 153730. [CrossRef] [PubMed]
5. Evode, N.; Qamar, S.A.; Bilal, M.; Barceló, D.; Iqbal, H.M.N. Plastic Waste and Its Management Strategies for Environmental Sustainability. *Case Stud. Chem. Environ. Eng.* **2021**, *4*, 100142. [CrossRef]

6. Blanchard, R.; Mekonnen, T.H. Valorization of Plastic Waste via Chemical Activation and Carbonization into Activated Carbon for Functional Material Applications. *RSC Appl. Polym.* **2024**, *2*, 557–582. [CrossRef]
7. Bhattacharya, R. A Review on Production and Application of Activated Carbon from Discarded Plastics in the Context of 'Waste Treats Waste'. *J. Environ. Manag.* **2023**, *325*, 116613. [CrossRef] [PubMed]
8. Cansado, I.P.D.P.; Mourão, P.A.M.; Nabais, J.M.V.; Tita, B.; Batista, T.; Rocha, T.; Borges, C.; Matos, G. Use of Dirty Plastic Waste as Precursors for Activated Carbon Production—A Contribution to the Circular Economy. *Water Environ. J.* **2022**, *36*, 96–104. [CrossRef]
9. Kumari, M.; Chaudhary, G.R.; Chaudhary, S.; Umar, A. Transformation of Solid Plastic Waste to Activated Carbon Fibres for Wastewater Treatment. *Chemosphere* **2022**, *294*, 133692. [CrossRef]
10. Ligero, A.; Calero, M.; Pérez, A.; Solís, R.R.; Muñoz-Batista, M.J.; Martín-Lara, M.Á. Low-Cost Activated Carbon from the Pyrolysis of Post-Consumer Plastic Waste and the Application in CO_2 Capture. *Process Saf. Environ. Prot.* **2023**, *173*, 558–566. [CrossRef]
11. Pereira, L.; Castillo, V.; Calero, M.; Blázquez, G.; Solís, R.R.; Martín-Lara, M.Á. Insights into Using Plastic Waste to Produce Activated Carbons for Wastewater Treatment Applications: A Review. *J. Water Process Eng.* **2024**, *62*, 105386. [CrossRef]
12. Pérez-Huertas, S.; Calero, M.; Ligero, A.; Pérez, A.; Terpiłowski, K.; Martín-Lara, M.A. On the Use of Plastic Precursors for Preparation of Activated Carbons and Their Evaluation in CO_2 Capture for Biogas Upgrading: A Review. *Waste Manag.* **2023**, *161*, 116–141. [CrossRef] [PubMed]
13. Chew, T.W.; H'Ng, P.S.; Luqman Chuah Abdullah, B.C.T.G.; Chin, K.L.; Lee, C.L.; Mohd Nor Hafizuddin, B.M.S.; TaungMai, L. A Review of Bio-Based Activated Carbon Properties Produced from Different Activating Chemicals during Chemicals Activation Process on Biomass and Its Potential for Malaysia. *Materials* **2023**, *16*, 7365. [CrossRef]
14. Williams, P.T.; Reed, A.R. Development of Activated Carbon Pore Structure via Physical and Chemical Activation of Biomass Fibre Waste. *Biomass Bioenergy* **2006**, *30*, 144–152. [CrossRef]
15. Gao, Y.; Yue, Q.; Gao, B.; Li, A. Insight into Activated Carbon from Different Kinds of Chemical Activating Agents: A Review. *Sci. Total Environ.* **2020**, *746*, 141094. [CrossRef]
16. Karume, I.; Bbumba, S.; Tewolde, S.; Mukasa, I.Z.T.; Ntale, M. Impact of Carbonization Conditions and Adsorbate Nature on the Performance of Activated Carbon in Water Treatment. *BMC Chem.* **2023**, *17*, 162. [CrossRef]
17. Ilyas, M.; Ahmad, W.; Khan, H. Utilization of Activated Carbon Derived from Waste Plastic for Decontamination of Polycyclic Aromatic Hydrocarbons Laden Wastewater. *Water Sci. Technol.* **2021**, *84*, 609–631. [CrossRef]
18. Heidarinejad, Z.; Dehghani, M.H.; Heidari, M.; Javedan, G.; Ali, I.; Sillanpää, M. Methods for Preparation and Activation of Activated Carbon: A Review. *Environ. Chem. Lett.* **2020**, *18*, 393–415. [CrossRef]
19. Illingworth, J.M.; Rand, B.; Williams, P.T. Understanding the Mechanism of Two-Step, Pyrolysis-Alkali Chemical Activation of Fibrous Biomass for the Production of Activated Carbon Fibre Matting. *Fuel Process. Technol.* **2022**, *235*, 107348. [CrossRef]
20. Maulina, S.; Anwari, F.N. Comparing Characteristics of Charcoal and Activated Carbon from Oil Palm Fronds. *IOP Conf. Ser. Earth Environ. Sci.* **2019**, *305*, 012059. [CrossRef]
21. Zhu, C.; Pundienė, I.; Pranckevičienė, J.; Kligys, M. Effects of Na_2CO_3/Na_2SiO_3 Ratio and Curing Temperature on the Structure Formation of Alkali-Activated High-Carbon Biomass Fly Ash Pastes. *Materials* **2022**, *15*, 8354. [CrossRef] [PubMed]
22. Pereira, L.; Castillo, V.; Calero, M.; Blázquez, G.; Solís, R.R.; Martín-Lara, M.Á. Conversion of Char from Pyrolysis of Plastic Wastes into Alternative Activated Carbons for Heavy Metal Removal. *Environ. Res* **2024**, *250*, 118558. [CrossRef] [PubMed]
23. Hanum, F.; Bani, O.; Izdiharo, A.M. Characterization of Sodium Carbonate (Na_2CO_3) Treated Rice Husk Activated Carbon and Adsorption of Lead from Car Battery Wastewater. *IOP Conf. Ser. Mater. Sci. Eng.* **2017**, *180*, 012149. [CrossRef]
24. Bazan-Wozniak, A.; Nosal-Wiercińska, A.; Yilmaz, S.; Pietrzak, R. Chitin-Based Porous Carbons from Hermetia Illucens Fly with Large Surface Area for Efficient Adsorption of Methylene Blue; Adsorption Mechanism, Kinetics and Equilibrium Studies. *Measurement* **2024**, *226*, 114129. [CrossRef]
25. Liamprawat, T.; Verasarut, P.; Kaewtrakulchai, N.; Panomsuwan, G.; Chutipaijit, S.; Puengjinda, P.; Fuji, M.; Eiad-Ua, A. Synthesis of Porous Carbon Materials from Water Hyacinth via Hydrothermal Carbonization Assisted Chemical Activation for Carbon-Based Electrode Applications. *AIP Conf. Proc.* **2020**, *2279*, 130004. [CrossRef]
26. Zhang, J.; Zhang, W.; Zhang, H.; Pang, J.; Cao, G.; Han, M.; Yang, Y. Facile Preparation of Water Soluble Phenol Formaldehyde Resin-Derived Activated Carbon by Na_2CO_3 Activation for High Performance Supercapacitors. *Mater. Lett.* **2017**, *206*, 67–70. [CrossRef]
27. Komljenović, M.; Baščarević, Z.; Bradić, V. Mechanical and Microstructural Properties of Alkali-Activated Fly Ash Geopolymers. *J. Hazard. Mater.* **2010**, *181*, 35–42. [CrossRef]
28. Doussang, L.; Samson, G.; Deby, F.; Huet, B.; Guillon, E.; Cyr, M. Durability Parameters of Three Low-Carbon Concretes (Low Clinker, Alkali-Activated Slag and Supersulfated Cement). *Constr. Build. Mater.* **2023**, *407*, 133511. [CrossRef]
29. Alvarez, J.; Lopez, G.; Amutio, M.; Bilbao, J.; Olazar, M. Upgrading the Rice Husk Char Obtained by Flash Pyrolysis for the Production of Amorphous Silica and High Quality Activated Carbon. *Bioresour. Technol.* **2014**, *170*, 132–137. [CrossRef]

30. Maulina, S.; Handika, G.; Irvan; Iswanto, A.H. Quality Comparison of Activated Carbon Produced From Oil Palm Fronds by Chemical Activation Using Sodium Carbonate versus Sodium Chloride. *J. Korean Wood Sci. Technol.* **2020**, *48*, 503–512. [CrossRef]
31. Quan, C.; Wang, W.; Su, J.; Gao, N.; Wu, C.; Xu, G. Characteristics of Activated Carbon Derived from Camellia Oleifera Cake for Nickel Ions Adsorption. *Biomass Bioenergy* **2023**, *171*, 106748. [CrossRef]
32. Lall, A.S.; Pandey, A.K.; Mani, J.V. Pb (II) Adsorption over Activated Carbon Prepared from Cedrus Deodara Bark by Na_2CO_3 Activation: Optimal Design for Modelling and Process Optimization. *ChemistrySelect* **2024**, *9*, e202303143. [CrossRef]
33. Hao, Y.S.; Othman, N.; Zaini, M.A.A. Waste Newspaper as Cellulose Resource of Activated Carbon by Sodium Salts for Methylene Blue and Congo Red Removal. *Int. J. Biol. Macromol.* **2024**, *277*, 134353. [CrossRef] [PubMed]
34. Vijayaraghavan, K.; Ashokkumar, T. Characterization and Evaluation of Reactive Dye Adsorption onto Biochar Derived from Turbinaria Conoides Biomass. *Environ. Prog Sustain. Energy* **2019**, *38*, 13143. [CrossRef]
35. Gurung, M.; Hossain, M.Z.; Mumin, A.; Xu, W.Z.; Charpentier, P.A. Hemp Fibers Derived Porous Carbon for Naphthenic Acids Removal from Contaminated Aqueous Stream. *Biomass Convers. Biorefinery* **2024**. [CrossRef]
36. Salihu, R.; Abd Razak, S.I.; Ahmad Zawawi, N.; Rafiq Abdul Kadir, M.; Izzah Ismail, N.; Jusoh, N.; Riduan Mohamad, M.; Hasraf Mat Nayan, N. Citric Acid: A Green Cross-Linker of Biomaterials for Biomedical Applications. *Eur. Polym. J.* **2021**, *146*, 110271. [CrossRef]
37. Xie, N.; Chen, Z.; Wang, H.; You, C. Activated Carbon Coupled with Citric Acid in Enhancing the Remediation of Pb-Contaminated Soil by Electrokinetic Method. *J. Clean. Prod.* **2021**, *308*, 127433. [CrossRef]
38. Yao, X.; Liu, Y.; Li, T.; Zhang, T.; Li, H.; Wang, W.; Shen, X.; Qian, F.; Yao, Z. Adsorption Behavior of Multicomponent Volatile Organic Compounds on a Citric Acid Residue Waste-Based Activated Carbon: Experiment and Molecular Simulation. *J. Hazard. Mater.* **2020**, *392*, 122323. [CrossRef]
39. Chen, F.; Zhang, Y.; Zheng, M.; Xiao, Y.; Hu, H.; Liang, Y.; Liu, Y.; Dong, H. Preparation of High-Performance Porous Carbon Materials by Citric Acid-Assisted Hydrothermal Carbonization of Bamboo and Their Application in Electrode Materials. *Energy Fuels* **2022**, *36*, 9303–9312. [CrossRef]
40. Liu, L.; Fang, W.; Yuan, M.; Li, X.; Wang, X.; Dai, Y. Metolachlor-Adsorption on the Walnut Shell Biochar Modified by the Fulvic Acid and Citric Acid in Water. *J. Environ. Chem. Eng.* **2021**, *9*, 106238. [CrossRef]
41. Juengchareonpoon, K.; Wanichpongpan, P.; Boonamnuayvitaya, V. Graphene Oxide and Carboxymethylcellulose Film Modified by Citric Acid for Antibiotic Removal. *J. Environ. Chem. Eng.* **2021**, *9*, 104637. [CrossRef]
42. Nemati, F.; Jafari, D.; Esmaeili, H. Highly Efficient Removal of Toxic Ions by the Activated Carbon Derived from Citrus Limon Tree Leaves. *Carbon Lett.* **2021**, *31*, 509–521. [CrossRef]
43. Soldatkina, L.; Yanar, M. Equilibrium, Kinetic, and Thermodynamic Studies of Cationic Dyes Adsorption on Corn Stalks Modified by Citric Acid. *Colloids Interfaces* **2021**, *5*, 52. [CrossRef]
44. Martín-Lara, M.A.; Piñar, A.; Ligero, A.; Blázquez, G.; Calero, M. Characterization and Use of Char Produced from Pyrolysis of Post-Consumer Mixed Plastic Waste. *Water* **2021**, *13*, 1188. [CrossRef]
45. Solís, R.R.; Calero, M.; Pereira, L.; Ramírez, S.; Blázquez, G.; Martín-Lara, M.Á. Transforming a Mixture of Real Post-Consumer Plastic Waste into Activated Carbon for Biogas Upgrading. *Process Saf. Environ. Prot.* **2024**, *190*, 298–315. [CrossRef]
46. Dombrowski, R.J.; Lastoskie, C.M.; Hyduke, D.R. The Horvath–Kawazoe Method Revisited. *Colloids Surf. A Physicochem. Eng. Asp.* **2001**, *187–188*, 23–39. [CrossRef]
47. Gauden, P.A.; Terzyk, A.P.; Rychlicki, G.; Kowalczyk, P.; Ćwiertnia, M.S.; Garbacz, J.K. Estimating the Pore Size Distribution of Activated Carbons from Adsorption Data of Different Adsorbates by Various Methods. *J. Colloid Interface Sci.* **2004**, *273*, 39–63. [CrossRef]
48. *ISO 14040:2006*; Environmental Management—Life Cycle Assessment—Principles and Framework. ISO: Geneva, Switzerland, 2006.
49. *ISO 14044:2006*; Environmental Management—Life Cycle Assessment—Requirements and Guidelines. ISO: Geneva, Switzerland, 2006.
50. Sato, N.; Amano, Y.; Machida, M. Adsorption Characteristics of Nitrate Ion by Sodium Carbonate Activated PAN-Based Activated Carbon Fiber. *SN Appl. Sci.* **2022**, *4*, 315. [CrossRef]
51. Thommes, M.; Kaneko, K.; Neimark, A.V.; Olivier, J.P.; Rodríguez-Reinoso, F.; Rouquerol, J.; Sing, K.S.W.W. Physisorption of Gases, with Special Reference to the Evaluation of Surface Area and Pore Size Distribution (IUPAC Technical Report). *Pure Appl. Chem.* **2015**, *87*, 1051–1069. [CrossRef]
52. Chen, J.P.; Wu, S.; Chong, K.H. Surface Modification of a Granular Activated Carbon by Citric Acid for Enhancement of Copper Adsorption. *Carbon* **2003**, *41*, 1979–1986. [CrossRef]
53. Jiao, F.; Sang, H.; Guo, P.; Miao, P.; Wang, X. Efficient Adsorption and Porous Features from Activated Carbon Felts Activated by the Eutectic of Na_2CO_3 and K_2CO_3 with Vapor. *Chem. Phys. Lett.* **2022**, *803*, 139831. [CrossRef]

54. Kiliç, M.; Apaydin-Varol, E.; Pütün, A.E. Preparation and Surface Characterization of Activated Carbons from Euphorbia Rigida by Chemical Activation with $ZnCl_2$, K_2CO_3, NaOH and H_3PO_4. *Appl. Surf. Sci.* **2012**, *261*, 247–254. [CrossRef]
55. Mehdi, R.; Naqvi, S.R.; Khoja, A.H.; Hussain, R. Biomass Derived Activated Carbon by Chemical Surface Modification as a Source of Clean Energy for Supercapacitor Application. *Fuel* **2023**, *348*, 128529. [CrossRef]
56. Demir, M.; Doguscu, M. Preparation of Porous Carbons Using NaOH, K_2CO_3, Na_2CO_3 and $Na_2S_2O_3$ Activating Agents and Their Supercapacitor Application: A Comparative Study. *ChemistrySelect* **2022**, *7*, e202104295. [CrossRef]
57. Romero-Cano, L.A.; García-Rosero, H.; Carrasco-Marín, F.; Pérez-Cadenas, A.F.; González-Gutiérrez, L.V.; Zárate-Guzmán, A.I.; Ramos-Sánchez, G. Surface Functionalization to Abate the Irreversible Capacity of Hard Carbons Derived from Grapefruit Peels for Sodium-Ion Batteries. *Electrochim. Acta* **2019**, *326*, 134973. [CrossRef]
58. Liu, W.J.; Jiang, H.; Yu, H.Q. Development of Biochar-Based Functional Materials: Toward a Sustainable Platform Carbon Material. *Chem. Rev.* **2015**, *115*, 12251–12285. [CrossRef]
59. Cuthbertson, A.A.; Lincoln, C.; Miscall, J.; Stanley, L.M.; Maurya, A.K.; Asundi, A.S.; Tassone, C.J.; Rorrer, N.A.; Beckham, G.T. Characterization of Polymer Properties and Identification of Additives in Commercially Available Research Plastics. *Green Chem.* **2024**, *26*, 7067–7090. [CrossRef]
60. Chen, X.; Wang, X.; Fang, D. A Review on C1s XPS-Spectra for Some Kinds of Carbon Materials. *Fuller. Nanotub. Carbon Nanostruct.* **2020**, *28*, 1048–1058. [CrossRef]
61. Ramírez-Valencia, L.D.; Bailón-García, E.; Moral-Rodríguez, A.I.; Carrasco-Marín, F.; Pérez-Cadenas, A.F. Carbon Gels–Green Graphene Composites as Metal-Free Bifunctional Electro-Fenton Catalysts. *Gels* **2023**, *9*, 665. [CrossRef] [PubMed]
62. Burg, P.; Fydrych, P.; Cagniant, D.; Nanse, G.; Bimer, J.; Jankowska, A. The Characterization of Nitrogen-Enriched Activated Carbons by IR, XPS and LSER Methods. *Carbon* **2002**, *40*, 1521–1531. [CrossRef]
63. Rocha, R.P.; Pereira, M.F.R.; Figueiredo, J.L. Characterisation of the Surface Chemistry of Carbon Materials by Temperature-Programmed Desorption: An Assessment. *Catal. Today* **2023**, *418*, 114136. [CrossRef]
64. Jarvis, P.; Fawell, J. Lead in Drinking Water—An Ongoing Public Health Concern? *Curr. Opin. Environ. Sci. Health* **2021**, *20*, 100239. [CrossRef]
65. Foo, K.Y.; Hameed, B.H. Insights into the Modeling of Adsorption Isotherm Systems. *Chem. Eng. J.* **2010**, *156*, 2–10. [CrossRef]
66. Mozaffari Majd, M.; Kordzadeh-Kermani, V.; Ghalandari, V.; Askari, A.; Sillanpää, M. Adsorption Isotherm Models: A Comprehensive and Systematic Review (2010−2020). *Sci. Total Environ.* **2022**, *812*, 151334. [CrossRef]
67. Al-Ghouti, M.A.; Da'ana, D.A. Guidelines for the Use and Interpretation of Adsorption Isotherm Models: A Review. *J. Hazard. Mater.* **2020**, *393*, 122383. [CrossRef] [PubMed]
68. Uçar, S.; Erdem, M.; Tay, T.; Karagöz, S. Removal of Lead (II) and Nickel (II) Ions from Aqueous Solution Using Activated Carbon Prepared from Rapeseed Oil Cake by Na_2CO_3 Activation. *Clean Technol. Environ. Policy* **2015**, *17*, 747–756. [CrossRef]
69. Kuo, C.Y.; Wu, C.H.; Chen, M.J. Adsorption of Lead Ions from Aqueous Solutions by Citric Acid-Modified Celluloses. *Desalination Water Treat.* **2015**, *55*, 1264–1270. [CrossRef]
70. Yang, X.; Flowers, R.C.; Weinberg, H.S.; Singer, P.C. Occurrence and Removal of Pharmaceuticals and Personal Care Products (PPCPs) in an Advanced Wastewater Reclamation Plant. *Water Res.* **2011**, *45*, 5218–5228. [CrossRef] [PubMed]
71. Wu, J.L.; Liu, Z.H.; Ma, Q.G.; Dai, L.; Dang, Z. Occurrence, Removal and Risk Evaluation of Ibuprofen and Acetaminophen in Municipal Wastewater Treatment Plants: A Critical Review. *Sci. Total Environ.* **2023**, *891*, 164600. [CrossRef] [PubMed]
72. Lima, D.R.; Hosseini-Bandegharaei, A.; Thue, P.S.; Lima, E.C.; de Albuquerque, Y.R.T.; dos Reis, G.S.; Umpierres, C.S.; Dias, S.L.P.; Tran, H.N. Efficient Acetaminophen Removal from Water and Hospital Effluents Treatment by Activated Carbons Derived from Brazil Nutshells. *Colloids Surf. A Physicochem. Eng. Asp.* **2019**, *583*, 123966. [CrossRef]
73. Wong, S.; Lim, Y.; Ngadi, N.; Mat, R.; Hassan, O.; Inuwa, I.M.; Mohamed, N.B.; Low, J.H. Removal of Acetaminophen by Activated Carbon Synthesized from Spent Tea Leaves: Equilibrium, Kinetics and Thermodynamics Studies. *Powder Technol.* **2018**, *338*, 878–886. [CrossRef]
74. Paredes-Laverde, M.; Salamanca, M.; Silva-Agredo, J.; Manrique-Losada, L.; Torres-Palma, R.A. Selective Removal of Acetaminophen in Urine with Activated Carbons from Rice (*Oryza sativa*) and Coffee (*Coffea arabica*) Husk: Effect of Activating Agent, Activation Temperature and Analysis of Physical-Chemical Interactions. *J. Environ. Chem. Eng.* **2019**, *7*, 103318. [CrossRef]
75. Gatrouni, M.; Asses, N.; Bedia, J.; Belver, C.; Molina, C.B.; Mzoughi, N. Acetaminophen Adsorption on Carbon Materials from Citrus Waste. *J. Carbon Res.* **2024**, *10*, 53. [CrossRef]
76. Pramanik, P.; Patel, H.; Charola, S.; Neogi, S.; Maiti, S. High Surface Area Porous Carbon from Cotton Stalk Agro-Residue for CO_2 Adsorption and Study of Techno-Economic Viability of Commercial Production. *J. CO2 Util.* **2021**, *45*, 101450. [CrossRef]
77. Amin, M.; Shah, H.H.; Iqbal, A.; Farooqi, Z.U.R.; Krawczuk, M.; Zia, A. Conversion of Waste Biomass into Activated Carbon and Evaluation of Environmental Consequences Using Life Cycle Assessment. *Appl. Sci.* **2022**, *12*, 5741. [CrossRef]

78. Pereira, P.H.F.; Maia, L.S.; da Silva, A.I.C.; Silva, B.A.R.; Pinhati, F.R.; de Oliveira, S.A.; Rosa, D.S.; Mulinari, D.R. Prospective Life Cycle Assessment Prospective (LCA) of Activated Carbon Production, Derived from Banana Peel Waste for Methylene Blue Removal. *Adsorption* **2024**, *30*, 1081–1101. [CrossRef]
79. Amin, M.; Chung, E.; Shah, H.H. Effect of Different Activation Agents for Activated Carbon Preparation through Characterization and Life Cycle Assessment. *Int. J. Environ. Sci. Technol.* **2023**, *20*, 7645–7656. [CrossRef]